Construction and Building Materials 236 (2020) 117581

Contents lists available at ScienceDirect

Construction and Building Materials

journal homepage: www.elsevier.com/locate/conbuildmat

Capillary suction induced water absorption and chloride transport in non-saturated concrete: The influence of humidity, mineral admixtures and sulfate ions

Chang Honglei [a], Jin Zuquan [b,*], Zhao Tiejun [b], Wang Benzhen [b], Li Zhe [b], Liu Jian [a]

[a] School of Qilu Transportation, Shandong University, Jinan 250002, China
[b] Engineering Research Center of Concrete Technology in Marine Environment, Ministry of Education, Qingdao University of Technology, Qingdao 26033, China

HIGHLIGHTS

- Seawater and NaCl-Na_2SO_4 composite solution are used as the aggressive solution in experiments.
- Water absorption and chloride transport induced by short time capillary suction are characterized.
- Influence of internal humidity, mineral admixtures, and sulfate ions are discussed.
- Relation between water absorption and chloride penetration under short time capillary suction condition are evaluated.

ARTICLE INFO

Article history:
Received 27 April 2019
Received in revised form 9 September 2019
Accepted 10 November 2019

Keywords:
Concrete
Water absorption
Chloride
Capillary suction

ABSTRACT

Concrete structures in marine environments are gravely jeopardized by chloride attack caused by capillary suction. To investigate the erosion of concrete induced by capillary suction under various factors, seawater and NaCl-Na_2SO_4 solution were used as corrosive solution to obtain the evolution law of water absorbed amount and chloride content in concrete with different water to binder ratio, fly ash and slag dosages and internal relative humidity. The results show that the decrease of internal relative humidity leads to the increase of seawater absorbed by capillary suction in a brief period, and boost rapid growth of chloride content in surface of concrete. For early age (28 d) concrete specimens, when the fly ash dosage is 0–30% or the slag dosage is 0–50%, the water absorption rate and chloride content of concrete are more likely to drop with the dosage increasing. Furthermore, under short-time capillary suction condition, SO_4^{2-} has a minor impact on water absorption of concrete, while slightly increases the chloride content. However, the chloride content does not evolve coincidently with the change of SO_4^{2-} concentration. Moreover, within a brief exposure period, the chloride content linearly develops with absorbed sweater amount, and it is inappropriate to use chloride diffusion coefficient to reflect the chloride transport rate of concrete under capillary absorption effect.

1. Introduction

There is a huge amount of corrosive ions in seawater, such as chloride ions and sulfate ions. When concrete structures are exposed to marine environments, those corrosive ions will heavily devastate their durability and safety [1–4]. For instance, if chlorides penetrate to steel surface and exceed a certain concentration, they will initiate steel corrosion accompanied by water and oxygen [5,6]. And with increasing of chloride concentration, the steel corrosion will be accelerated, which can lead to concrete crack and shorten the service life of concrete structures [7,8].

When concrete is in marine submersion zone, chlorides enter the matrix mainly through diffusion. Instead, while in splash or tidal zone, concrete is usually unsaturated, and chlorides transport into concrete first through capillary suction and then penetrate deeper position through diffusion. Different from diffusion, capillary suction can directly absorb seawater into concrete, raise surface chloride content rapidly and hence increases the probability of steel corrosion [9–11]. Therefore, it is of great significance to investigate the water absorption of unsaturated concrete and the corresponding chloride distribution resulted, which can provide

* Corresponding author.
E-mail address: jinzuquan@126.com (J. Zuquan).

https://doi.org/10.1016/j.conbuildmat.2019.117581
0950-0618/

solid foundation for the durability design and service life evaluation of concrete structures under marine environments.

Among the present studies about capillary suction, many are concerned with the influence of varied factors on water absorption of concrete. It is well-known that the water absorption is highly dependent on pore structure and water content of concrete [12–14]. And the essential of different factors affecting that is to change the pore structure and moisture distribution. Therefore, studies about factors influencing water absorption can generally be divided into two categories: one focuses on pore structure, and the other focus on moisture content.

For studies on factors that can vary pore structure of concrete, the experimental results of Liu [15] showed that the water absorption rate (WAR) of concrete decreased with water to binder ratio (W/B) and dosage of fly ash (FA) or silica fume (SF), and the reduction of WAR was doubled when the FA and SF are mixed together in concrete. The effect of W/B was also investigated by Safiuddin [16], and test results revealed that the water absorption decreased with lower W/B ratio. According to test results of Leung [17], a remarkable reduction in WAR was found when cement was partially replaced by only FA. And same as the results of Liu, the effect of combined use of FA and SF on decreasing WAR was much more significant than using FA only. Meanwhile, increasing the dosage of FA or SF leaded to an enhanced reduction of WAR. Walid [18] observed lower WAR for blast furnace slag (SL) substitution when its dosages are less than 40%. And Liu [19] reported that WAR of concrete decreased with the increasing of SL content when its dosage was less than 50%. Moreover, Razak [20] and Guneyisi [21] investigated the WAR of concrete blended with metakaolin (MK) and SF, and the results showed that the presence of MK and SF significantly reduced WAR of concrete. It can be concluded that, the water absorption of concrete decreases with the mixing of mineral admixtures and the decline of W/B, and the decrease rate heavily depends on the amount of dosage.

As to studies about the effect of moisture content on water absorption of concrete, in the study of Parrlott [22], concrete specimens were dried and conditioned at 50 °C oven to obtain a uniform moisture distribution prior to testing for WAR of concrete. And the test results for a range of concretes showed that WAR was very sensitive to the internal relative humidity (IRH) of matrix. Mohammadi [23] also discovered that water absorption is strongly affected by IRH, and his results showed that water absorption increased significantly with the decreasing of IRH. Furthermore, Li [24] found a close relationship between water absorption and saturation degree of concrete. And Yang [25,26] investigated the influence of different saturation degree on water absorption of concrete, and found that the WAR decreased with saturation degree increasing. Consisting with the above finding, the studies of Zhang [27] and Chang [28] also found that saturation degree was closely related to water absorption of concrete, the lower the saturation degree, the greater the WAR, and thus more solution could be absorbed during water absorbing process. Besides, Kato [29] examined the influence of the initial saturation degree on the permeability of sodium chloride solution into mortar specimens, and revealed that the permeability distance of the solution increased with the decreasing of the initial saturation degree.

Most of the previous studies use either water or salt solution rather than seawater as soak solution to explore the influence of different factors on the water absorption of concrete. The constitution of seawater is very complicated, containing many kinds of corrosive ions. And the density of seawater also differs from water or salt solution. The adoption of seawater can better reveal the water absorption of concrete in actual marine environments and need more related studies. Besides, sulfate ion is also another main corrosive ion in seawater, and whether sulfate ion content have an effect on water absorption and chloride distribution in concrete under capillary suction condition within a short-time is still undefined, which also needs further investigation.

Considering the wide use of mineral admixtures in marine engineering and the shifting humidity in marine environments, this study plans to build different internal humidity spaces in concrete, test water absorbed amount and chloride content of concrete mixed with different dosages of FA and SL using seawater and NaCl-Na_2SO_4 solution as soak solution, and explore influence of these factors on water absorption and chloride penetration from perspectives of pore structure, water content and ions.

2. Experiment programs

2.1. Raw materials and sample preparation

The P.O 42.5 Portland cement produced by Shandong Shanshui Co., Ltd. was used in this study. The mineral admixtures are FA and SL. The FA used is Luqing grade I and the SL is grade S95, whose fineness meet GB/T 1596-2005 standard. The chemical composition of cement and mineral admixtures are shown in Table 1. The coarse aggregate is crude gravel with diameter being 5–20 mm, and the fine aggregate is good grading river sand with 2.5 fineness modulus. The water-reducing agent is the polycarboxylate superplasticizer produced by Jiangsu Sobute New Materials Co., Ltd.

This study designed concretes with different W/B, different dosages of gel material, and different dosages of fly ash and slag. The mix proportions of concrete are presented in Table 2. The W/B is 0.35 and 0.45, and the gel material dosage is 450 kg/m^3, 435 kg/m^3, and 352 kg/m^3. For concretes with 450 kg/m^3 dosage of gel material, the cement were partially replaced by fly ash and slag, with the FA replacement ratio being 15%, 30%, and 50% and the SL replacement ratio being 15%, 30%, 50%, 65% successively.

After concrete was properly mixed and tested the workability, they were filled in the moulds with size being 100 mm × 100 mm × 100 mm, and the surface of moulds was sealed with thin film and tape to prevent moisture evaporation. Concrete specimens were demoulded after 24 h' hardening and cured in a room (temperature being 23 ± 2 °C and relative humidity being above 95%) for 3 d, 7 d, 28 d, and 56 d separately.

2.2. Compressive strength test

The compressive strength of concretes with different mixes (L50–L53, F51–F54, U1, and U2) and curing time (3 d, 7 d, 28 d, and 56 d) were tested using a press machine, and the results are presented in Table 2. It can be observed that compressive stress increases with the increase of curing time, gel material dosage and decrease of W/B. When the FA dosage is 15% and 30%, it can improve the compressive stress of concrete, while when its dosage is 50%, the compressive stress of concrete decreases significantly at early curing age. When the SL dosage is 15% and 30%, it can increase the compressive strength of concrete, while when its dosage is 50% and 65%, the compressive stress of concrete decreases at early curing age. However, with the increase of curing time, the compressive strength of concrete blended with large dosage of FA and SL develops and approaches or even surpasses that of concrete without mineral admixtures at 56d.

2.3. Construction of internal humidity space

Different internal humidity spaces of concrete were built in four ways with specimens being placed in water, constant temperature and humidity room, 45 °C oven, and saturated LiBr solution in a closed vessel. More specially, 12 specimens cured for 28 d were divided into 4 groups and each group has 3 specimens. Those spec-

Table 1
Chemical composition of P.O 42.5 Cement, FA and SL (%wt).

Chemical composition	SiO_2	Al_2O_3	Fe_2O_3	CaO	MgO	TiO_2	Na_2O	K_2O	SO_3
Cement (%)	20.1	5.09	2.93	61.7	1.58	0.340	0.700	0.360	1.99
FA	45.4	36.3	5.30	6.97	0.599	1.65	0.314	0.864	1.24
SL	29.0	12.5	1.30	46.3	5.72	0.570	0.560	0.320	1.18

Table 2
Concrete mixes (kg/m^3).

NO.	W/B	Cement	SL	FA	Sand	Gravel	Water	Superplasticizer	Compressive strength/MPa				Workability/mm
									3d	7d	28d	56d	
L50	0.35	450	0	0	711	1067	155	5.4	32.9	39.5	48.2	53.0	185
L51	0.35	382.5	0	67.5	711	1067	155	5.4	47.1	53.4	63.3	72.0	240
L52	0.35	315	0	135	711	1067	155	5.4	37.7	41.9	52.9	58.2	240
L53	0.35	225	0	225	711	1067	155	5.4	1.80	2.05	25.6	32.9	185
F51	0.35	382.5	67.5	0	711	1067	155	5.4	35.1	40.7	56.3	58.1	240
F52	0.35	315	135	0	711	1067	155	5.4	34.7	36.1	57.7	58.5	210
F53	0.35	225	225	0	711	1067	155	5.4	26.8	35.6	53.8	55.1	230
F54	0.35	157.5	292.5	0	711	1067	155	5.4	23.9	26.4	44.1	47.8	240
U1	0.45	352	0	0	653	1214	158	3.5	28.5	31.3	38.9	43.4	230
U2	0.35	435	0	0	565	1143	156	4.3	29.4	35.4	41.8	46.9	210

imens were cut in half along the middle line (shown in Fig. 1). Note that the cutting surface is the exposed surface, and the other five surfaces were sealed with epoxy resin before the following treatments. The epoxy resin was completely hardened after curing for 2 days, and then all the samples were fully saturated in a vacuum water tank, and dried in a 45 °C oven. 3 groups of these specimens were taken out from the oven after completely dried and then were placed in water, constant humidity and temperature room, and saturated LiBr solution environment mentioned above. The IRH of these specimens were monitored in real time through the prebuilt humidity sensor (10 mm from the exposed surface). Meanwhile, the other group was always placed in a 45 °C oven and monitored the IRH at the same depth as that of the other specimens. When the IRH of specimens under four conditions reached 100% (water immersion), 65% (constant temperature and humidity room), 55% (45 °C oven), and 31% (saturated LiBr solution in a closed vessel) separately, specimens were taken out and conducted the water absorption test.

2.4. Water absorption test

Specimens after internal humidity building were put on the brackets placed in the bottom of a plastic box, with the exposed surface downward. Next, seawater (obtained from Qingdao marine exposure station and its composition is presented in Table 3) or NaCl-Na_2SO_4 solution was poured into the box until the liquid level is 3–5 mm above the bottom of specimens, shown in Fig. 2. The mass of specimens was tested at absorption time 0 h, 1 h, 2 h, 3 h, 4 h, 5 h, 6 h, 7 h, 8 h, 9 h, 10 h, 11 h, and 12 h successively, and the evolution law of absorbed seawater amount induced by capillary suction was thus obtained. Moreover, the capillary absorption coefficient can be gained through Eq. (1).

Note that seawater was used as aggressive solution in this study to investigate the influence of different factors on water absorption and chloride distribution, aiming to reflect the field situation of concrete structures in marine environments. Meanwhile, based on chloride concentration in the seawater, a range of NaCl-Na_2SO_4 corrosive solution were also prepared to explore the influence of SO_4^{2-} concentration on water absorption and chloride penetration. The NaCl content in NaCl-Na_2SO_4 solution was constantly 3.5%, and the Na_2SO_4 content was 0.2%, 0.5%, 1.0%, 1.62%, and 1.75% successively. Note that, except those specimens designed for studying the influence of IRH and exposure time, the IRH of all other specimens was controlled to be 65% and the water absorption time was 12 h.

$$\Delta W = A\sqrt{t} \tag{1}$$

where, ΔW is the amount of absorbed water per unit area of concrete, mg/cm^2; A is the capillary absorption coefficient, $mg/(cm^2\ h^{1/2})$; t is the water absorption time, h.

2.5. Chloride content test

After reaching the water absorption time, a milling machine was used to grind powder from specimens layer by layer starting from the exposed surface. Powder samples at different depths of specimens were obtained. Within the depth range 0–10 mm, the grinding interval is 2 mm, while in the depth range 10–28 mm,

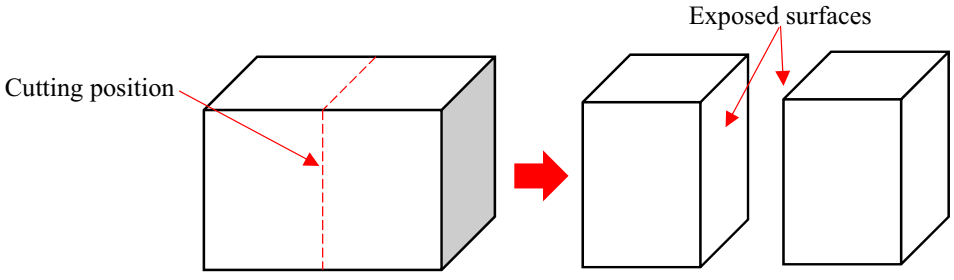

Fig. 1. Illustration of cutting position and exposed surfaces in the specimen.

Table 3
Composites and corrosion properties of seawater in the marine exposure field.

Constituent	Ion content mg/L							pH	salinity%
	NO_3^-	HCO_3^-	SO_4^{2-}	Cl^-	NH_4^+	Ca^{2+}	Mg^{2+}		
Sea water	12.76	161.29	2176.12	17533.33	<0.04	407.83	1177.38	8.2	3.5

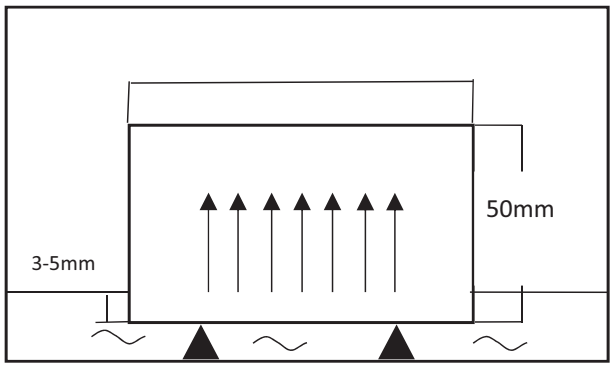

Fig. 2. Illustration of water absorption test.

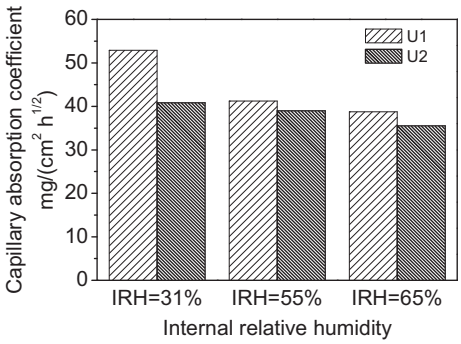

Fig. 4. Capillary absorption coefficients of concretes with different IRH.

the grinding interval is 3 mm, 5 mm, and 10 mm successively. In this study, since chloride ions penetrated into concrete driven by capillary suction in a very short time, it was hard to form bound chloride or the formed bound chloride was very limited in this process. Therefore, only free chloride content was tested. The silver nitration titration method was employed to test free chloride in compliance with the ASTM C1152 [30,31].

3. Results and discussion

3.1. Factors influencing water absorption of concrete

3.1.1. IRH

Fig. 3 shows the evolution law of water absorbed amount per unit area of concrete with different IRH, and Fig. 4 presents the corresponding capillary absorption coefficient. It can be seen from Fig. 3 that the amount of absorbed water increases with square root of time in a linear trend abiding by Eq. (1). It can also be observed that the lower the IRH is, the higher the amount of absorbed water is and so is the capillary absorption coefficient (see Fig. 4). For unsaturated concrete, the main drive of water absorption is capillary suction whose strength is highly dependent on IRH [28,32]. It can be seen from Eq. (2) that the capillary suction force becomes stronger when IRH get lower, which will boost the absorbed water content and WAR within the same time.

$$\Delta p = -\frac{RT\rho_l \cos\theta}{M} \ln RH \tag{2}$$

where, Δp is capillary suction force; RH is the relative humidity; M is the molar mass of liquid; θ is the contact angle; R is the ideal gas constant; ρ_l is the density of liquid; T is the temperature.

Besides, comparing the water absorption curve and coefficients of U1 and U2, it can be found that the decrease of W/B can lead to the decline of water absorbed amount and absorption rate. The reason is obvious that the lower the W/B is, the denser the concrete matrix is, which makes it harder for seawater to enter the matrix with other conditions being the same. Moreover, the difference among the three curves of U2 in Fig. 3(b) is smaller than that of U1 in Fig. 3(a), which is also caused by the denser matrix of U2.

3.1.2. Mineral admixtures

Fig. 5(a) and (b) show the evolution law of water absorbed amount per unit area of concrete with and without FA and SL, and Fig. 6 presents the corresponding capillary absorption coefficients. From Fig. 5(a), it can be found that water absorbed amount of specimens with different FA dosages linearly increases with time abiding by the square root law. When the FA dosage is 15% and 30%, the WAR decreases a bit compared with that of reference

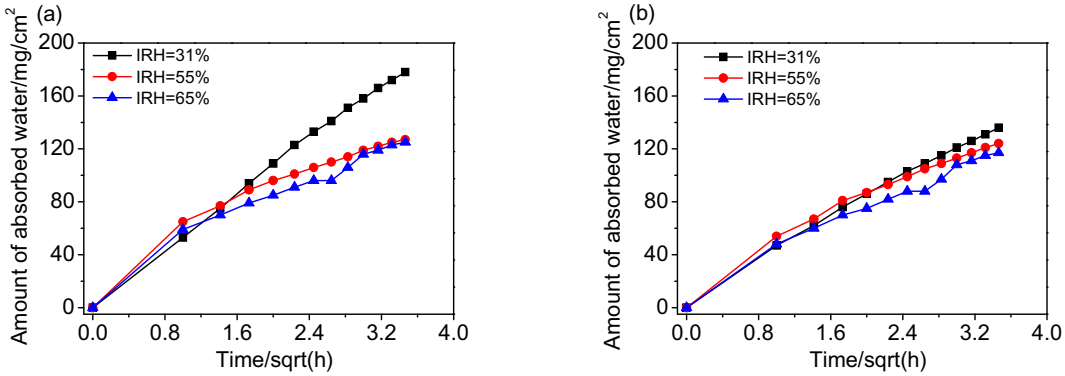

Fig. 3. The evolution law of water absorbed amount per unit area of concrete with different IRH: (a) U1 (b) U2.

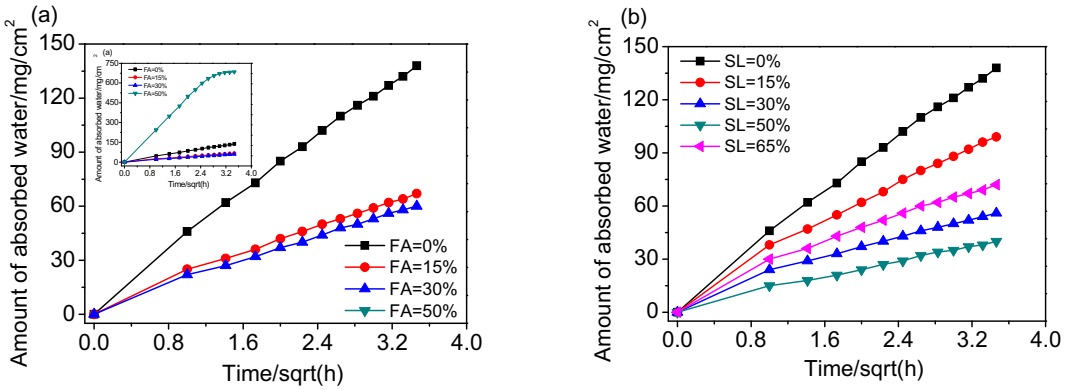

Fig. 5. The evolution law of water absorbed amount per unit area of concrete with different dosages of FA and SL: (a) FA (b) SL.

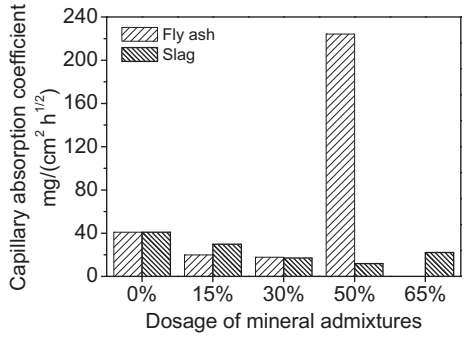

Fig. 6. Capillary absorption coefficients of concretes with different dosages of FA and SL.

specimens, and the WAR reduction of 30% FA specimens is only slightly higher than that of 15% FA specimens. However, when the FA dosage is 50%, the WAR rises dramatically (see Fig. 6), which is apparently related to the impact of FA on pore structure of matrix. The partial replacement of cement by FA compacts pore structure of concrete due to micro-aggregate filling effect of FA, while retards the development of pore structure resulted from the decrease of hydration degree at early age (because the pozzolanic effect of FA mainly functions at later stage, which though can guarantee of sustainable development of concrete strength (Table 2), decreases the hydration degree of concrete at early age [33–35]). Therefore, the compactness change of concrete blended with FA depends on the compromising between its positive and negative effects. As is shown in Fig. 5(a) and Fig. 6, the decrease of the WAR of concretes with 15% FA is prominent, while when the FA dosage increases to 30%, the WAR does not continue to decrease remarkably. It is obvious that when the FA dosage is low, its positive effect is stronger, and when its dosage increases, the negative effect dominates. It should be noted that the water absorption testing in this study was performed using concrete specimens at early age (28 d). If the age of concrete is large, like more than 1 year, the admixture of FA will have limited negative effect on the pore structure of concrete, and even the use of high volume FA will be more likely to decrease WAR.

From Fig. 5(b), it can be observed that the water absorbed amount per unit area of concrete with SL also increases with time in a square root trend. And combining Fig. 6, it can be found that except for concretes with 65% SL, the higher the SL dosage is, the lower the WAR of concrete. Similar to the effect of FA on concrete, SL also has both positive and negative impacts. However, researches [36–38] have revealed that when the dosage of SL is low, the heat release rate of cement-slag composite binder at early age approximates that of neat cement, while only when the SL dosage is high, the heat release rate of composite binder is significantly lower than that of neat cement, and this has been widely recognized. Therefore, the influence of SL on the decrease of hydration degree is much smaller than that of FA at the early age, which explains why only when the SL dosage reaches 65%, the WAR starts to grow but still is lower than that of concretes without SL.

In this study, seawater was used as aggressive solution to investigate the influence of FA or SL on the water absorption property of concrete, aiming to reveal the field situation of concrete structures in marine environments. Based on the results above, it can be inferred that no matter FA or SL, their dosage should not be too much in practice and should be preferably controlled within 30% and 50% respectively, especially for the concrete that has been in service since the early age. Otherwise, when concretes with FA or SL are exposed to marine environments, the durability and safety of concrete structures will be heavily jeopardized as more corrosive ions are introduced along with a large amount of seawater absorbed by capillary suction.

3.1.3. SO_4^{2-} concentration

Fig. 7 shows the evolution law of water absorbed amount per unit area of concrete exposed to NaCl-Na_2SO_4 solution with different SO_4^{2-} concentration, and Fig. 8 presents the corresponding capillary absorption coefficients. It is obvious that the water absorbed amount increases with time in a square-root trend. Meanwhile, combining Figs. 7 and 8, it can be found that, except that the water absorbed amount of specimens exposed to 0.5% Na_2SO_4 solution is lower than that of 0% Na_2SO_4 solution, the water adsorbed amount of all other specimens exposed to Na_2SO_4 solution is higher. Therefore, the mixing of Na_2SO_4 generally increases water adsorbed amount. However, the water absorbed amount dose not evolve accordingly with SO_4^{2-} concentration increasing. Moreover, the water absorbed amount of specimens in solution with different SO_4^{2-} concentration differs slightly within the same exposure time, suggesting that SO_4^{2-} probably has a minor influence on water absorption driven by capillary suction in a short time. According to Eqs. (2) and (3), the capillary suction force mainly depends on the radius of capillary pores and internal humidity of concrete. Thus, the capillary adsorption force generated is theoretically the same for the test specimens with the same pore structure and internal humidity. And the weight of NaCl-Na_2SO_4 solution absorbed within the same time should be the same under the identical short-time capillary suction condition, even if the density of NaCl-Na_2SO_4 solution increases with the rising of Na_2SO_4 content.

$$\Delta p = \frac{2\gamma\cos\theta}{r} \tag{3}$$

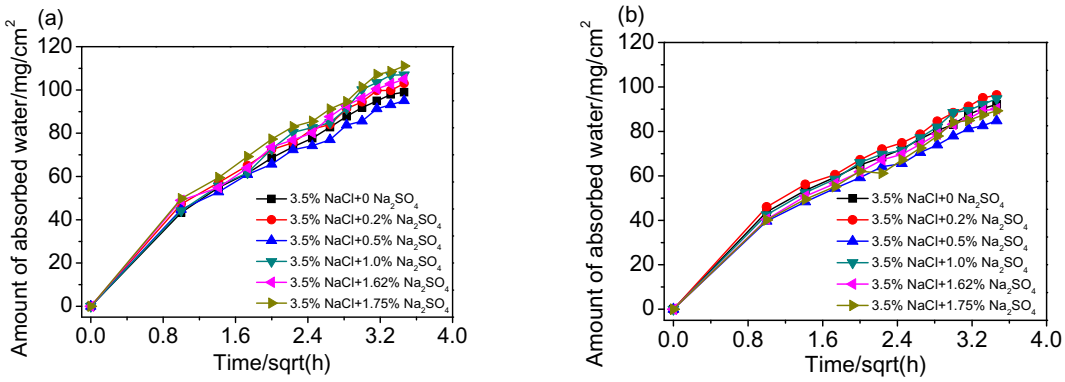

Fig. 7. The evolution law of water absorbed amount per unit area of concrete exposed to NaCl-Na_2SO_4 solution with different SO_4^{2-} concentration: (a) U1 (b) U2.

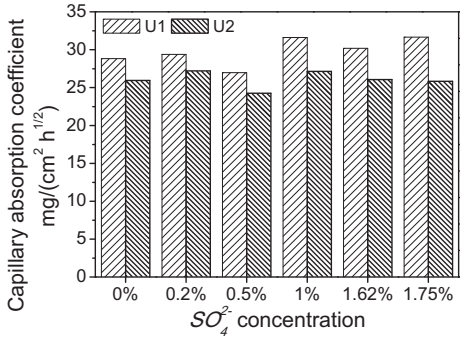

Fig. 8. Capillary absorption coefficients of concretes exposed to NaCl-Na_2SO_4 solution with different SO_4^{2-} concentration.

where, r is the radius of capillary pore, γ is the gas-liquid interfacial tension.

3.2. Factors influencing chloride distribution of concrete

3.2.1. IRH

Fig. 9 presents the chloride profiles of specimens U1 with different IRH. It can be observed that chloride content all decreases with the distance from the exposed surface increasing. For the saturated specimens (IRH = 100%), their chloride profiles are flat, and it can be ascribed to that diffusion is the major drive for chlorides to enter concrete from seawater in the absorption experiment. Consequently, no matter the exposure time is 1 h (Fig. 9(a) or 12 h (Fig. 9 (b)), chlorides that penetrated into matrix are very limited. For unsaturated specimens, the slope of chloride profiles are comparatively steep. The chloride content within 0–4 mm (1 h) and 0–8 mm (12 h) is very high, and then reaches a constant value at depths greater than 15 mm. The above phenomenon is apparently caused by capillary suction which introduces seawater into matrix in a brief period, leading to the high chloride content at places from surface to where water front reaches and very low chloride content beyond that range. It can also be found from Fig. 9 that, the lower the IRH of concrete is, the higher the chloride content at the same depth, which is especially tenable near the surface. From the above, it can be inferred that the amount of seawater absorbed by capillary suction increases with the IRH of concrete decreasing, contributing to the promotion of chloride content. Besides, comparing Fig. 9(a) and (b), it can be found that the chloride content of specimens with the same IRH is higher after longer exposure.

Fig. 10 shows the chloride distribution of specimens U2 with different IRH. It can be observed that the evolution law of chloride content of U2 is similar to that of U1, and the chloride content of U2 is lower than that of U1 with the same absorption time, IRH, and depth since the W/B of U2 is lower. Besides, according to chloride profiles in Figs. 9 and 10, the chloride front reaches at least 6 mm from the exposed surface after absorption for 1 h, and the chloride front reaches at least 10 mm after 12 h. Moreover, the lower the IRH is, the greater the chloride attack span is.

Note that in the field situation, instead of uniformly distributed, the internal humidity of concrete is the function of depth, which is the difference between this study and field situation. This study presents the worst result, and these data are obtained using seawater, which have an important reference value for the durability evaluation of concrete structures in field.

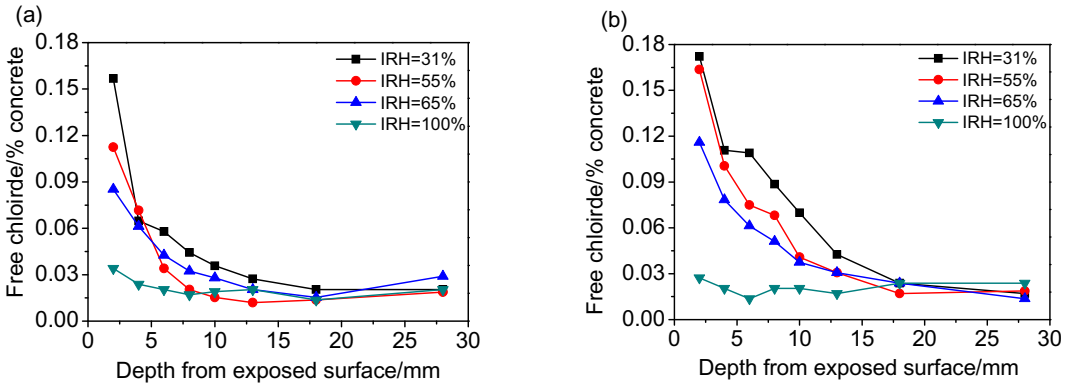

Fig. 9. The chloride distribution of specimens U1 with different IRH: (a) water absorption time 1 h (b) water absorption time 12 h.

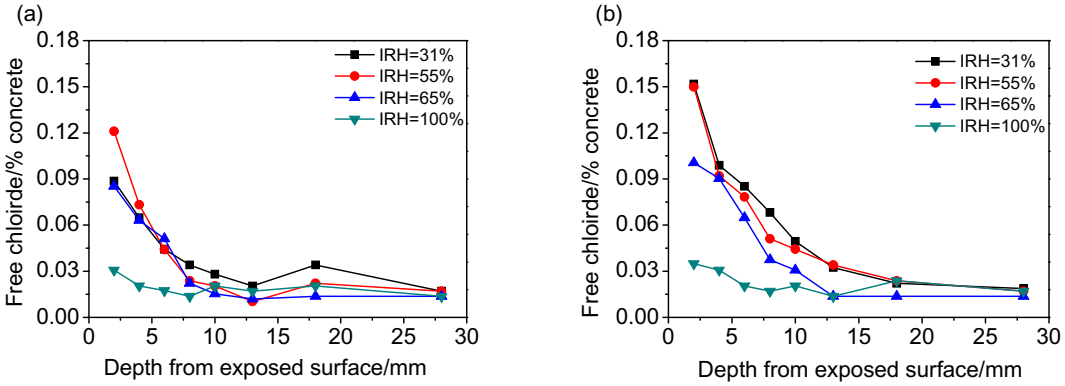

Fig. 10. The chloride distribution of specimens U2 with different IRH: (a) water absorption time 1 h (b) water absorption time 12 h.

3.2.2. Mineral admixtures

Fig. 11(a) and (b) present chloride profiles of concrete with different dosages of FA and SL. It can be seen that chloride content all decreases with depth from the exposed surface increasing, and the chloride content within 0–6 mm is high while decreases rapidly in deeper position. It can be found in Fig. 11(a) that, when the FA dosage is 15% and 30%, the corresponding chloride content drops significantly compared with that of specimens without FA. And when the dosage is 50%, the chloride content increases prominently and remains high throughout the whole test range. From Fig. 11(b), it can be observed that all different dosages of SL can lead to the drop of chloride content, and the higher the SL dosage, the more significant the decrease, excluding 65%. The impact of FA and SL on chloride distribution in concrete depends on their comprehensive effect on pore structure. It is known from the above that pore structure change contributes to the amount variation of absorbed seawater, which decides chloride distribution.

Moreover, as shown in Fig. 11, chlorides can easily penetrate into 0–10 mm from the exposed surface of specimens without mineral admixtures, which gravely jeopardizes the safety of concrete structures. However, with appreciate amount of mineral admixtures, the chloride attack range can be shortened to 0–6 mm, which is of great importance for the improvement of the durability of concrete structures. It is vital, though, the dosage of FA or SL should be controlled within a reasonable range; otherwise, it will be counterproductive.

3.2.3. SO_4^{2-} concentration

The chloride distribution of specimens U1 and U2 subjected to NaCl-Na_2SO_4 solution with different SO_4^{2-} concentration is shown in Fig. 13. It can be observed that chloride content generally decreases with distance from the exposed surface increasing. From Fig. 12(a), it can be seen that the mixing of SO_4^{2-} generally boosts the chloride content at corresponding depths compared with pure NaCl solution. However, the chloride content dose not evolve accordingly with SO_4^{2-} concentration increasing. For instance, the chloride content of concrete exposed to 0.5% SO_4^{2-} concentration is higher than that of 0.2% SO_4^{2-} concentration; but when the SO_4^{2-} concentration reaches 1.0%, the chloride content declines; while SO_4^{2-} concentration reaches 1.62%, chloride content increases again. Moreover, it can be seen from Fig. 12(b) that the chloride distribution of U2 is similar to that of U1. The chloride content of specimens exposed to solution mixed with SO_4^{2-} are generally a little higher than that exposed to pure NaCl solution, but still there is not a regular change law between chloride content and SO_4^{2-} concentration. In addition, since the W/B of U2 is smaller than that of U1, chloride content of the former are all lower than that of the latter with the same condition.

Some studies [39–41] have reported that that the presence of SO_4^{2-} can accelerate chloride attack, and in these studies, the migration of ions is dominantly driven by prolonged diffusion. Under such condition, both the chemical reactions with hydrates and the charge interaction between ions play an important role on aggravating chloride erosion. However, the migration of ions in this study is driven by capillary suction in a very short period, which leads to limited effect of the above chemical reactions and charge interaction. Furthermore, according to the experimental results and analysis of Section 3.1.3, the difference in weight of serial NaCl-Na_2SO_4 solution absorbed by specimens is quite small. Thus the volume of the solution entering the matrix decreases as the Na_2SO_4 content increases, because the density of NaCl-Na_2SO_4 solution increases with Na_2SO_4 content rising. Therefore, for specimens with the same pore structure, the solution with larger Na_2SO_4 content will be relatively concentrated in shallower position of matrix, while the solution with smaller Na_2SO_4 content will be relatively more dispersed along the vertical depth. And thereby, the mixing of Na_2SO_4 in NaCl solution causes a slight increase of chloride content in surface layer of concrete, which is basically consistent with the experimental results of U1 and U2. Besides, the influence of SO_4^{2-} concentration on chloride transport induced by capillary suction is complicated and the reason for that is still unclear, which needs more investigations.

3.3. Relation between water absorption and chloride penetration

Under short-time capillary suction condition, chloride content of concrete is definitely dependent on the seawater amount absorbed into matrix. In this part, the quantitative relation between them is established through linking the water absorbed amount of concrete after exposure for 12 h to the chloride content within the test range calculated through Eq. (4) based on chloride profiles, shown in Fig. 13. It can be observed that the chloride content increases with seawater absorbed amount, presenting a good linear correlation with the slope being 1.44×10^{-4}.

$$C_{0\ x_t} = \sum \frac{x_b - x_a}{x_t} \cdot C_{x_a\ x_b} \tag{4}$$

where, $C_{0\ x_t}$ is the chloride content per unit mass of concrete within the whole test range; $C_{x_a\ x_b}$ is the chloride content in depth x_a–x_b of chloride profiles; x_t is the total test depth, 28 mm; x_a, x_b is the testing depth, 0, 2, 4, 6, 8, 10, 13, 18 mm of x_a, and 2, 4, 6, 8, 10, 13, 18, 28 mm of x_b.

In this study, chloride ions in concrete are mainly introduced by capillary suction. As a result, it is not accurate in theory to obtain the chloride diffusion coefficient through fitting the error function (Eq. (5)) of Fick's second law with chloride profiles. Therefore, it is

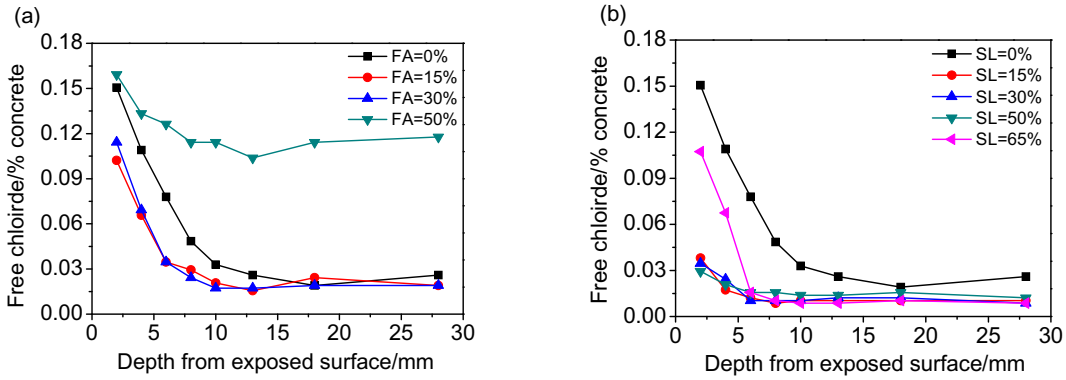

Fig. 11. The chloride distribution of concretes with different dosages of FA and SL: (a) FA (b) SL.

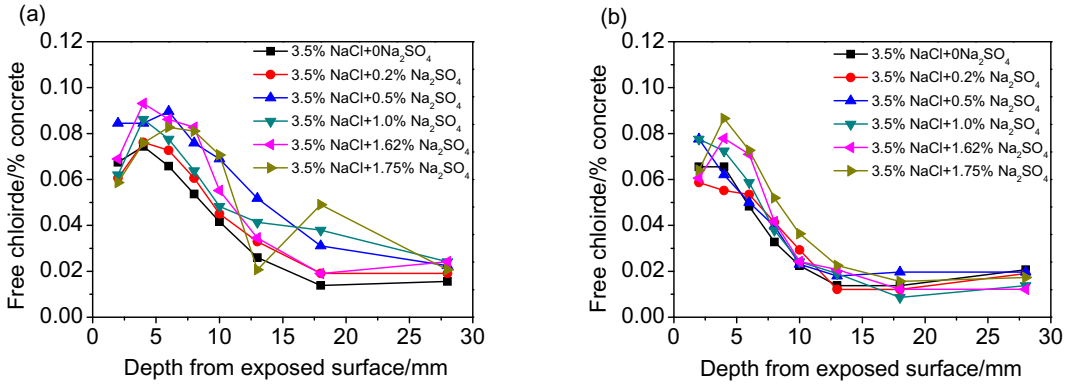

Fig. 12. The chloride distribution of concretes exposed to NaCl-Na_2SO_4 solution with different SO_4^{2-} concentration: (a) U1 (b) U2.

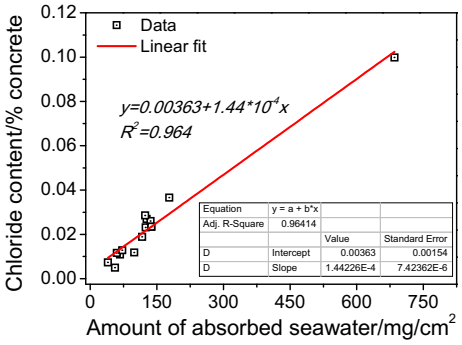

Fig. 13. Quantitative relation between seawater absorbed amount and chloride content.

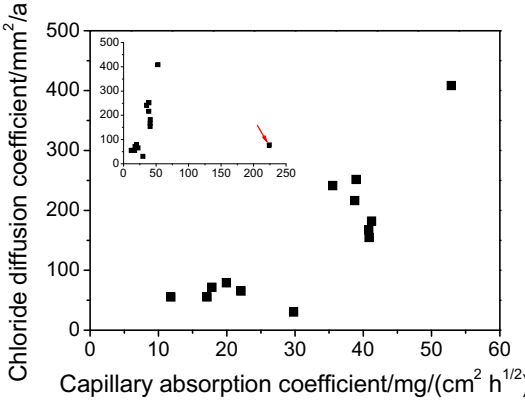

Fig. 14. Quantitative relation between capillary absorption coefficients and chloride diffusion coefficients.

still pending about whether it is feasible to evaluate the chloride transport rate using diffusion coefficient in this study. Actually, the chloride transport rate in this situation is closely related to the WAR of concrete. And thereby, this part tries to analyze the relation between capillary absorption coefficient and chloride diffusion coefficient in order to evaluate the feasibility and accuracy of using diffusion coefficient to reflect chloride transport rate. The correlation between them of corresponding specimens and conditions is presented in Fig. 14. The inset image on the top left of Fig. 14 shows the distribution of all data points, and the point indicated by the red arrow obviously violates the overall evolution of data points. That point corresponds to the specimen with 50% FA, and the real situation for this specimen is that its WAR is the biggest and its chloride content is highest, which is contradicted with the chloride diffusion coefficient obtained by Eq. (5). As shown in Fig. 11(a), the chloride content of 50%FA specimens is very large within the whole test depth. However, the difference between the surface chloride content and chloride content at depth 28 mm is not very large, which results in a smaller diffusion coefficient. Therefore, for this group of specimens, it is inappropriate to simply use diffusion coefficient to reflect chloride transport rate under capillary adsorption condition. Zooming in the x-coordinate by 0–60, the evolution of other data is more distinct. It can be found that, though the chloride diffusion coefficient generally increases with capillary absorption coefficient, their local correspondence is chaotic and not qualified for representing their quantitative relation. Therefore, under short-time capillary suction condition, chloride diffusion coefficient cannot properly reflect the chloride transport rate in concrete.

$$C_{(x,t)} = C_0 + (C_s - C_0)\left(1 - erf\left[\frac{x}{2\sqrt{Dt}}\right]\right) \quad (5)$$

where, $C_{(x,t)}$ is the chloride content at depth of x and time of t; C_s is the surface chloride content; C_0 is the initial chloride content; D is the chloride diffusion coefficient obtained using tradition method; x is the distance from the exposed surface; t is exposure time.

4. Conclusions

1) The decrease of IRH leads to the increase of absorbed seawater amount under short-time capillary suction condition, which results in rapid increase of chloride content in surface of concrete.
2) For early age (28d) concrete specimens, when the FA dosage is 0–30% or the SL dosage is 0–50%, both the WAR and chloride content of concrete are more likely to drop with the dosage increasing. While when their dosage further increases beyond that range, WAR and chloride content may start to grow and surpass that of specimens without mineral admixtures.
3) Under short-time capillary suction condition, SO_4^{2-} has a minor impact on WAR of concrete, while slightly increases the chloride content. However, the chloride content does not evolve coincidently with the change of SO_4^{2-} concentration.
4) Within the same exposure time, the chloride content linearly develops with the amount of absorbed seawater, and it is inappropriate to use chloride diffusion coefficient to represent the chloride transport rate of concrete under short-time capillary suction condition.

Declaration of Competing Interest

The authors declare that they have no known competing financial interests or personal relationships that could have appeared to influence the work reported in this paper.

Acknowledgements

This work is a part of a series of projects financially supported by the National Natural Science Foundation of China (No. 51908327, 51678318 and No. 51420105015), the National Basic Research Program of China (973 Program) (No. 2015CB655100), the Natural Science Foundation of Shandong Province (No. ZR2019QEE017) and the Fundamental Research Funds of Shandong University (No. 31560078614117). Besides, this work is also supported by National 111 project. All these supports are gratefully appreciated.

References

[1] B. Hwan-Oh, S. Yup Jang, Effects of material and environmental parameters on chloride penetration profiles in concrete structures, Cem. Concr. Res. 37 (1) (2007) 47–53.
[2] Honglei Chang, Chloride binding capacity of pastes influenced by carbonation under three conditions, Cem. Concr. Compos. 84 (2017) 1–9.
[3] Penggang Wang, Yuting Jia, Tao Li, Dongshuai Hou, Qi Zheng, Molecular dynamics study on ions and water confined in the nanometer channel of Friedel's salt: structure, dynamics and interfacial interaction, Phys. Chem. Chem. Phys. 20 (2018) 27049–27058.
[4] Q.F. Liu, G.L. Feng, J. Xia, J. Yang, L.Y. Li, Ionic transport features in concrete composites containing various shaped aggregates: a numerical study, Compos. Struct. 183 (2018) 371–380.
[5] Z. Li, Z.Q. Jin, T.J. Zhao, P.G. Wang, Z.J. Li, C.S. Xiong, K.L. Zhang, Use of a novel electro-magnetic apparatus to monitor corrosion of reinforced bar in concrete, Sensor. Actuat. A-Phys. 286 (2019) 14–27.
[6] Guojian Liu, Yunsheng Zhang, Ziwei Ni, Ran Huang, Corrosion behavior of steel submitted to chloride and sulphate ions in simulated concrete pore solution, Constr. Build. Mater. 115 (2016) 1–5.
[7] Honglei Chang, Pan Feng, Kai Lyu, Jian Liu, A novel method for assessing C-S-H chloride adsorption in cement pastes, Constr. Build. Mater. 225 (2019) 324–331.
[8] X.H. Shen, W.Q. Jiang, D. Hou, Z. Hu, J. Yang, Q.F. Liu, Numerical study of carbonation and its effect on chloride binding in concrete, Cem. Concr. Compos. (2019), https://doi.org/10.1016/j.cemconcomp.2019.103402.
[9] D. Conciatori, H. Sadouki, E. Brühwiler, Capillary suction and diffusion model for chloride ingress into concrete, Cem. Concr. Res. 38 (2008) 1401–1408.
[10] Honglei Chang, Mu. Song, Pan Feng, Influence of carbonation on "maximum phenomenon" under cyclic wetting and drying condition, Cem. Concr. Res. 103 (2018) 95–109.
[11] Guojian Liu, Yunsheng Zhang, Wu. Meng, Ran Huang, Study of depassivation of carbon steel in simulated concrete pore solution using different equivalent circuits, Constr. Build. Mater. 157 (2017) 357–362.
[12] C. Hall, Water sorptivity of mortars and concretes: a review, Mag. Concr. Res. 41 (147) (1989) 51–61.
[13] N.S. Martys, C.F. Ferraris, Capillary transport in mortars and concrete, Cem. Concr. Res. 27 (5) (1997) 747–760.
[14] X.H. Shen, Q.F. Liu, Z. Hu, W.Q. Jiang, X. Lin, D. Hou, P. Hao, Combine ingress of chloride and carbonation in marine-exposed concrete under unsaturated environment: a numerical study, Ocean. Eng. (2019) 106350.
[15] Liu Wei, Xing Feng, Xie Youjun, Influence of mineral admixture on the water sorptivity of concrete, J. Shenzhen Uni. Sci. Eng. 25 (2008) 303–307.
[16] Md. Safiuddin, J.S. West, K.A. Soudki, Hardened properties of self-consolidating high performance concrete including rice husk ash, Cem. Concr. Compos. 32 (9) (2010) 708–717.
[17] H.Y. Leung, J. Kim, A. Nadeem, J. Jaganathan, M.P. Anwar, Sorptivity of self-compacting concrete containing fly ash and silica fume, Constr. Build. Mater. 113 (2016) 369–375.
[18] D. Walid, O.M. Nadjib, B. Abderrazak, B. Larbi, Effect of incorporating blast furnace slag and natural pozzolana on compressive strength and capillary water absorption of concrete, in: The 7th Scientific-technical Conference on Material Problems in Civil Engineering, 2015, pp. 254–261.
[19] Baoju Liu, Guo Luo, Youjun Xie, Effect of curing conditions on the permeability of concrete with high volume mineral admixtures, Constr. Build. Mater. 167 (2018) 359–371.
[20] H. Abdul Razak, H.K. Chai, H.S. Wong, Near surface characteristics of concrete containing supplementary cementing materials, Cem. Concr. Compos. 26 (2004) 883–889.
[21] E. Guneyisi, M. Gesoglu, S. Karaoglu, K. Mermerdas, Strength, permeability and shrinkage cracking of silica fume and metakaolin concretes, Constr. Build. Mater. 34 (2012) 120–130.
[22] L.J. Parrlott, Moisture conditioning and transport properties of concrete test specimens, Mater. Struct. 27 (1994) 460–468.
[23] Mohammadi Babak, Nokken Michelle, Mirvalad Sajjad, Development of in situ water absorption method: laboratory study and field validation, J. Mater. Civ. Eng. 29 (10) (2017). 04017182.
[24] Li Wenting, Mohammad Pour-Ghaz, Castro Javier, Water absorption and critical degree of saturation relating to freeze-thaw damage in concrete pavement joints, J. Mater. Civ. Eng. 24 (3) (2012) 299–307.
[25] Lin Yang, Danying Gao, Yunsheng Zhang, Jiyu Tang, Ying Li, Relationship between sorptivity and capillary coefficient for water absorption of cement-based materials: theory analysis and experiment, Royal Soc. Open Sci. 6 (2019) 190112.
[26] Lin Yang, Danying Gao, Yunsheng Zhang, Wei She, Study on water and chloride transport in cracked mortar using X-ray CT, gravimetric method and natural immersion method, Constr. Build. Mater. 176 (2018) 652–664.
[27] Qinghang Zhang, Gu. Xianglin, Weiping Zhang, Qinghua Hung, Model on capillary pressure-saturation relationship for concrete, J. Tongji Univ. (Natural Sci.) 40 (12) (2012) 1753–1759.
[28] Honglei Chang, Mu. Song, Deqing Xie, Penggang Wang, Influence of pore structure and moisture distribution on chloride "maximum phenomenon" in surface layer of specimens exposed to cyclic drying-wetting condition, Constr. Build. Mater. 131 (2017) 16–30.
[29] Y. Kato, Y. Ikeda, S. Naomachi, E. Kato, An experimental study on the influence of initial degree of saturation in mortar on water absorption of mortar with containing chloride ion, in: Life-Cycle Civil Engineering Systems: Emphasis on Sustainable Civil Infrastructure, 2017, pp. 1983–1988.
[30] Y. Jiang, Z. Jin, T. Zhao, Y. Chen, F.X. Chen, Strain field of reinforced concrete under accelerated corrosion by digital image correlation technique, J. Adv Concr Technol. 15 (2017) 290–299.
[31] Honglei Chang, Pan Feng, Jian Liu, Zuquan Jin, Kai Lv, Qiaoling Liu, Chloride maximum phenomenon near the surface of cement paste induced by moisture evaporation and carbonation, Mater. Struct. 51 (5) (2018).
[32] Wei Sun, Changwen Miao, Modern Concrete Theory and Technology, Science Press, Beijing, 2012, pp. 196–199.
[33] I. Pane, W. Hansen, Investigation of blended cement hydration by isothermal calorimetry and thermal analysis, Cem. Concr. Res. 35 (6) (2005) 1155–1164.
[34] J.W. Bullard, H.M. Jennings, R.A. Livingston, A. Nonat, G.W. Scherer, J.S. Schweitzer, K.L. Scrivener, J.J. Thomas, Mechanisms of cement hydration, Cem. Concr. Res. 41 (12) (2011) 1208–1223.

[35] D.G. Snelson, S. Wild, M. O'Farrell, Heat of hydration of portland cement–metakaolin–fly ash (PC–MK–PFA) blends, Cem. Concr. Res. 38 (6) (2008) 832–840.
[36] Zhonghe Shui, Xiaosheng Wei, Dongmin Wang, Modern Concrete Science and Technology, Science Press, Beijing, 2014, pp. 120–123.
[37] A. Bougara, C. Lynsdale, N.B. Milestone, The influence of slag properties, mix parameters and curing temperature on hydration and strength development of slag/cement blends, Constr. Build. Mater. 187 (2018) 339–347.
[38] O.R. Ogirigbo, L. Black, Influence of slag composition and temperature on the hydration and microstructure of slag blended cements, Constr. Build. Mater. 126 (2016) 496–507.
[39] Shukai Cheng, Zhonghe Shui, Xu Tao Sun, Cheng Gao, Effects of sulfate and magnesium ion on the chloride transportation behavior and binding capacity of Portland cement mortar, Constr. Build. Mater. 204 (2019) 265–275.
[40] Yuanzhang Cao, Liping Guo, Bo Chen, Influence of sulfate on the chloride diffusion mechanism in mortar, Constr. Build. Mater. 197 (2019) 398–405.
[41] Fouzia Shaheen, Bulu Pradhan, Effect of chloride and conjoint chloride–sulfate ions on corrosion of reinforcing steel in electrolytic concrete powder solution (ECPS), Constr. Build. Mater. 101 (2015) 99–112.